ASIAN JOURNAL OF PHARMACEUTICAL SCIENCES 12 (2017) 569–579

Available online at www.sciencedirect.com

ScienceDirect

journal homepage: www.elsevier.com/locate/ajps

Original Research Paper

Bioenhanced advanced third generation solid dispersion of tadalafil: Repurposing with improved therapy in pyelonephritis

Prashant P. Mande, Sagar S. Bachhav, Padma V. Devarajan *

Department of Pharmaceutical Sciences and Technology, Institute of Chemical Technology, N. P. Marg, Matunga (E), Mumbai, Maharashtra, India

ARTICLE INFO

Article history:
Received 31 January 2017
Received in revised form 12 April 2017
Accepted 2 July 2017
Available online 3 August 2017

Keywords:
Phosphodiesterase-5
Lipopolysaccharide
Kidney infection
Eudragit EPO
Kidney failure

ABSTRACT

Tadalafil (TDL) a BCS-II drug is recently reported for repurposing nephroprotective effect in Pyelonephritis (PN). However, poor water solubility and dissolution rate limited oral bioavailability pose serious challenges in its therapeutic applications. We present an advanced third generation Solid Dispersion (SD) of TDL comprising a polymer in combination with a Self Micro-emulsifying Composition (SMEC) to achieve high drug loading, improved stability and rapid dissolution of TDL for enhancing bioavailability and efficacy in PN. TDL-SMEC-SD was coated onto rapidly disintegrating inert tablet cores which disintegrated rapidly in water to release SD as a film. TDL-SMEC-SD was evaluated for *in-vivo* oral bioavailability and *in-vivo* efficacy in lipopolysaccharide-induced PN in rats. TDL exhibited high solubility (45.6 mg/ml) in the SMEC. TDL-SMEC-SD exhibited remarkably high TDL loading (45%w/w), exceptionally low contact angle (9°), rapid in-vitro release (t_{50} 7.3 min), microemulsion formation (globule size ~100 nm) in aqueous dispersion, and stability as per ICH guidelines. SEM, DSC, and XRD confirmed high physical stability. A relative bioavailability of 350% and 150% compared to TDL and TDL-SD without SMEC respectively, established the superiority of TDL-SMEC-SD. A significant reduction in serum creatinine, blood urea nitrogen and nitric oxide levels in the lipopolysaccharide-induced PN confirmed the benefit of the TDL-SMEC-SD. The advanced third generation SMEC SDs presents the possibility of platform technology for bioenhancement of poorly water soluble drugs.

* *Corresponding author.* Department of Pharmaceutical Sciences and Technology, Institute of Chemical Technology, N. P. Marg, Matunga (E), Mumbai, Maharashtra, India. Tel.: + 91 22 33612201.
E-mail address: pvdevarajan@gmail.com (P.V. Devarajan).
Peer review under responsibility of Shenyang Pharmaceutical University.
https://doi.org/10.1016/j.ajps.2017.07.001

1. Introduction

Tadalafil (TDL), a phosphodiesterase-5 inhibitor is commonly used in the treatment of erectile dysfunction [1,2]. However, recently the protective effect of TDL in Pyelonephritis (PN), a kidney infection associated with severe inflammation, renal function deterioration, kidney failure and even death is demonstrated [3]. A rate limiting factor in the exploitation of TDL for clinical application is poor bioavailability and consequently limited clinical response, attributed to poor water solubility [4,5]. Enhancing solubility and dissolution rate of TDL is a prime requisite to ensure clinical efficacy. Repurposing TDL for PN therefore clearly spells the need for enhancing dissolution rates and solubility.

Complexation with cyclodextrins and coprocessing with Soluplus using high energy ball milling or supercritical carbon dioxide impregnation or inclusion of TDL in microporous silica was explored to enhance dissolution [4-7]. Nano-strategies evaluated include preparation of TDL nanocrystals or Self Nanoemulsifying Drug Delivery System (SNEDDS) for enhanced TDL solubility and dissolution rate [8,9].

Nonetheless, Solid Dispersions (SDs) present great promise for solubility and dissolution enhancement while providing readily scalable technology [10,11]. Second generation SDs comprises polymers for bioehancement, while third generation SDs contain a surfactant, in addition. A second generation TDL-SD using vinylpyrrolidone – vinyl acetate (PVA/VA) copolymer revealed limited enhancement in drug dissolution rate in comparison with crystalline TDL, while a third generation SDs of TDL comprising a polymeric surfactant, poloxamer 407 exhibited significant enhancement [12,13]. Nonetheless, a major limitation of these SDs is the restricted drug holding capacity and hence limited physical stability [14,15].

We have recently reported an advanced third generation SD as films, wherein the surfactant is replaced with a Self Microemulsifying Composition (SMEC), which enabled very high drug loading coupled with remarkable physical stability of the drug in the SD, and furthermore exhibited fourfold bioenhancement of Curcumin in rats [16]. In the present study, we report the development of an advanced third generation SD of TDL with the specific objective of evaluation for improved efficacy in a model of pyelonephritis.

2. Materials and method

2.1. Materials

TDL (Macleod's Pharmaceuticals, India), Capmul MCM and Captex 300 oil (Abitec Corporation India), Labrasol (Gattefosse, France), Eudragit EPO, Aerosil 200 (Evonik India PvtLtd), Kollidon VA 64 (KVA) (BASF India) and Hydroxypropyl methylcellulose (Methocel HPMC E5; Colorcon), Acetonitrile HPLC grade (Azeocryst Organics, India) were kindly supplied as gift samples. Tween 80 (Merck India), propylene glycol (Merck India), Magnesium Stearate (Signet chemicals Co Pvt Ltd), MCC 102 (FMC Pvt. Ltd), Lactose – Supertab 11 (FMC Pvt. Ltd), LPS(Sigma-Aldrich, USA), Griess reagent (Fluka Analytical), Vanadium (III)-chloride (Aldrich Chemistry), Serum creatinine kit (Accurex Biomedical Pvt. Ltd.), Blood urea nitrogen (BUN) kit (Agappe Diagnostic Ltd.), Acetone AR grade (S. D. fine chemicals) and Methanol HPLC grade (S. D. fine chemicals) were procured from respective manufacturer.

2.2. Optimization of SMEC for TDL: calculation of thermodynamic parameters

The affinity of TDL to the polymers and SMEC was assessed by calculating the following thermodynamic parameters.

2.2.1. Partial and total solubility parameters

The solubility parameter, based on the well-known rule of chemistry "like dissolves like", is a measure of the cohesive energy of a substance and hence an indicator of solute-solvent interaction. The total solubility parameter (δ_{total}) is calculated from partial solubility parameters associated with dispersion force, polar interaction and hydrogen bonding. Based on the knowledge of the specific substance's chemical structure, partial solubility parameters can be predicted by the method of group contribution [17]. Table 1 reports group

Table 1 – Solubility parameter component group contributions.

Structural Groups	F_d	$(F_p)^2$	E_h	V
-CH3	420	0	0	33.5
Phenyl	1270	12100	0	33.4
-O-	100	160000	3000	3.8
-OH	210	250000	20000	10.0
-CO-	290	592900	2000	10.8
=CH -	200	0	0	13.5
>C=	70	0	0	-5.5
-COO-	390	240100	7000	18
>N–	20	640000	5000	-9.0
$-CH_2-$	270	0	0	16.1
>CH–	80	0	0	-1.0
Ring	190	--	--	16
>C<	-70	0	0	-19.2

contributions taken from the literature [17]. Partial solubility parameters were calculated from the equations to give below.

The partial solubility parameter associated with dispersion forces δ_d is expressed as

$$\delta_d = \frac{\sum F_d}{\sum V}$$

The partial solubility parameter associated with polar interaction δ_p is expressed as

$$\delta_p = \frac{\sqrt{\sum F_p^2}}{\sum V}$$

The partial solubility parameter associated with hydrogen bonding δ_h is expressed as

$$\delta_h = \frac{\sqrt{\sum E_h}}{\sqrt{\sum V}}$$

F_d, F_p, E_h are the group contribution to dispersion forces, polar forces and hydrogen bond energy respectively, and V is the molar volume (Table 1).

From the partial solubility parameters, $\Delta\delta_{total}$ was calculated using Equation 1.

$$\delta_{total} = \sqrt{\delta_d^2 + \delta_p^2 + \delta_h^2} \quad (1)$$

2.2.2. *Calculation of mixing enthalpy*

The mixing enthalpy (ΔH_M), a thermodynamic parameter that reflects the energy required for mutual mixing of two components is an important parameter to correlate solute-solvent mixing. ΔH_M was calculated using Equation 2.

$$\Delta H_M = \Phi_1\Phi_2\left[(\delta_{d1} - \delta_{d2})^2 + (\delta_{p1} - \delta_{p2})^2 + (\delta_{h1} - \delta_{h2})^2\right] \quad (2)$$

Where Φ is molar volume fraction, while 1 and 2 represent solute and solvent respectively

2.2.3. *Calculation of polarity*

The polarity of a substance can be defined as follows to account the contribution from hydrogen bonding and other polar interactions and can be calculated from the Equation 3.

$$\text{Polarity} = 1 - \frac{\delta_d^2}{\delta_{total}^2} \quad (3)$$

Polarities of each component were calculated from Equation 3. The difference between polarities of two components (ΔPol) was calculated by subtracting the polarity of one component from other.

2.3. *Formulation of self microemulsifying composition (SMEC) of TDL*

2.3.1. *Preparation of SMEC*

The SMEC was prepared as described in our previous report [16]. Briefly, the oil (Capmul MCM - 20% w/w), surfactant (Tween 80 - 54% w/w) and co-surfactant (PEG - 26% w/w) were vortex mixed at room temperature. The solubility of TDL in 1 ml of SMEC was determined by addition of excess TDL with vortexing, till no more dissolved. After equilibration for 24h, the SMEC was centrifuged at 2000 rpm for 5 min and the supernatant evaluated for TDL by UV spectrophotometry at 285 nm. The solubility of TDL was also evaluated in the S/CoS mixture without the oil.

2.3.2. *Preparation of coating solution*

The polymers KVA/HPMC/Eudragit EPO (2% w/v) and SMEC (0.4% w/v) were dissolved in a solvent system comprising acetone: water (80:20) using an overhead stirrer for 0.5 h. The solubility of TDL in the polymeric solutions (1 ml) was determined by addition of TDL in incremental quantity till no more dissolved. Coating solutions were vortexed and allowed to stand for 10 min, centrifuged at 5000 rpm for 5 min and the supernatant evaluated for TDL by UV spectrophotometer at 285 nm using appropriate blank. Based on the solubility of TDL, solutions comprising polymer 1.0% w/v, SMEC 0.15%w/v and TDL 1.0%w/v were used for coating. A coating solution without SMEC was also evaluated.

2.3.3. *Free film study*

Free films were obtained by standard casting technique on glass slides. The films were observed under a polarizing microscope using IF550 filter at the the4x/0.13PhL lens (Olympus, Japan) for appearance and crystallization of TDL and images were captured.

2.3.4. *Preparation of TDL-SMEC-SD loaded tablets*

Inert core tablets comprising MCC 102 (49.5% w/w), Supertab 11 (49.5% w/w), Aerosil 200 (0.5% w/w) and magnesium stearate (0.5% w/w), were obtained by direct compression on a 16 station rotary tablet press. The excipients were mixed in a double cone blender (Shreeji Automachine, India) and compressed to tablets of ~250 mg using standard concave punches of 10 mm diameter. The Polymer, SMEC, and TDL dissolve in acetone: H_2O (80:20) were spray coated on inert tablet cores to obtain the SDs as polymeric films. SD equivalent to approximately ~20 mg of TDL/ tablet was readily coated using perforated coating pan (12-inch diameter) at the spray rate of 1–3 g/min and a pan speed of 6–7 rpm. The inlet and outlet temperature were maintained at 40–41 °C and 35–37 °C respectively. The SD variables evaluated include polymer type [KVA (KSM20), HPMC (HSM20) and Eudragit EPO (EPSM20)] where the number indicates the SMEC concentration in the SD as %w/w, and SMEC concentration in KVA as a polymer (KSM0, KSM10, KSM20 and KSM30). A barrier coat of HPMC 3%w/w was coated on the SDs by spraying HPMC (10%w/v) in acetone: water (80:20) to avoid sticking. Films comprising SMEC are referred to as TDL-SMEC-SD and films without SMEC as TDL-SD.

2.4. *Differential scanning calorimetric (DSC)*

TDL, polymers, TDL-SMEC-SDs and TDL-SD (5 mg) were taken in aluminum pans, sealed and subjected to differential scanning calorimetry under nitrogen flow using a Perkin Elmer Pyris 6 DSC thermal analysis instrument. Each sample was heated from 40 °C to 300 °C at a rate of 10 °C /min. Empty aluminum pan served as the reference.

2.5. X-ray diffraction (XRD)

XRD spectra of TDL, polymer (KVA), TDL-SMEC-SDs (KSM20) and TDL-SD (KSM0) were recorded at room temperature using Philips Pro Expert diffractometer, with nickel-filtered Cu Kα radiation at a voltage of 3 kV, 5 mA Current, 4° /min scanning speed, and 5°-70° (2θ) range.

2.6. Fourier transform infrared spectroscopy (FTIR)

FTIR spectra of TDL, polymers, TDL-SMEC-SD and TDL-SD were recorded on an infrared spectrometer (Perkin Elmer, Model spectrum RX) using the KBr pressed disc method. The scanning range was 400–4000 cm^{-1}.

2.7. Physicochemical characterization of tablets

Tablets were evaluated for assay, disintegration test, hardness and friability following standard methodology. Drug content was analyzed by HPLC using a mobile phase comprising 50 mM Sodium Dihydrogen Orthophosphate buffer (pH 3.0): Acetonitrile (47:53) at a flow rate 1.2 ml/min with a detection wavelength of 285 nm. HPLC analysis was performed on Jasco LC900 system equipped with Jasco PU-980 Intelligent HPLC pump, Jasco UV-975 Intelligent UV/VIS detector.

2.8. Scanning electron microscopy (SEM)

A tablet was mounted on the sample holder (stub) and sputtered with platinum using an auto fine coater and SEM micrographs of the tablets were obtained using an LV-SEM 5800 (JEOL, Japan) at an accelerating voltage of 10 kV.

2.9. Contact angle measurement

A drop of distilled water was carefully placed on the tablet surface and the contact angle was measured using Kruss contact angle apparatus (DSA-100, Krüss, Germany).

2.10. Microemulsion formation

TDL-SMEC-SD and TDL-SD coated tablets were placed in 200 ml of distilled water at room temperature (~28 °C) and allowed to disintegrate. The dispersions were subjected to mild agitation, filtered through a 0.45 μm membrane filter and the average droplet size and polydispersity index (PDI) determined to confirm the formation of the microemulsion. The size was determined by photon correlation spectroscopy using N4 plus submicron particle size analyzer (Beckman Coulter) at 25 °C.

2.11. In vitro drug release

In vitro dissolution of the TDL-SMEC-SD and TDL-SD was evaluated on the USP Type II apparatus, at 37 ± 5 °C and 50 rpm paddle speed in 900 ml of simulated gastric fluid (SGF, pH 1.2) without pepsin as dissolution medium. TDL powder was used as a reference. Samples (10 ml) were withdrawn at predetermined intervals up to 120 min and analyzed by UV spectrophotometry at 285 nm. Percent cumulative drug release versus time profiles was plotted. At the end of dissolution study filtered dissolution samples were also evaluated for average globule size and polydispersity index (PDI) by photon correlation spectroscopy using N4 plus submicron particle size analyzer (Beckman Coulter) at 25 °C. Data was analyzed using various dissolution kinetic models i.e. First-order, Zero order, Higuchi, Hixson–Crowell and Korsmeyer–Peppas.

2.12. Stability studies

TDL-SMEC-SD (KSM20) was evaluated for stability as per ICH guidelines. Tablets were packed in HDPE containers and stored at intermediate conditions [30 ± 2 °C, 65 ± 5% RH], and accelerated conditions [40 ± 2 °C, 75 ± 5% RH] and evaluated at regular time intervals for drug content and drug release. Tablets were also dispersed in water and filtered samples evaluated for globule size of the microemulsion.

2.13. In-vivo preclinical evaluation

2.13.1. Animals

Adult male Wistar rats (200 ± 20 g) were procured from Bombay Veterinary College, Mumbai, India. The rats were housed in polypropylene cages at an ambient temperature of 25 ± 1 °C and 45–55% RH, with a 12 h light/dark cycle. Standard rat chow pellets and water were allowed ad libitum. All the experimental procedures were approved by the Institutional Animal Ethics Committee (IAEC) of Institute of Chemical Technology, Mumbai (87/1999/ CPCSEA) and conducted as per the guidelines of Committee for the Purpose of Control and Supervision of Experiments on Animals (CPCSEA).

2.13.2. Pharmacokinetic study

The total of thirty-six rats were divided into three groups ($n = 12$ per group) and fasted for 8 h prior to the commencement of the study. The TDL-SMEC-SD (KSM20) and TDL-SD (KSM0) were dispersed in water before administration to rats. TDL suspension in 0.5% carboxymethylcellulose (group I), TDL-SMEC-SD (Group II), and TDL-SD (Group III) were administered to rats by oral gavage at the dose equivalent to TDL 10 mg/kg body weight. **S**parse sampling was performed using total 36 rats divided into the three main groups ($n = 12$), which were further divided into three subgroups ($n = 4$ per time point). The sparse sampling was performed for blood collection utilizing 4 rats per time point in each group. Hence, from each animal, blood was collected at maximum three-time points (0.5 ml/time point), which total to approximately 1.5 ml blood withdrawal from each rat. The blood samples (0.5 ml) were collected through retro-orbital plexus under isoflurane anesthesia at 0.25, 0.5, 1, 2, 4, 8, 12, 18 and 24 h post dosing into heparinized microcentrifuge tubes ($n = 4$). Plasma was separated by centrifugation at 10,000 rpm, 20 °C for 10 min and stored at −70 °C until TDL analysis.

A high-pressure liquid chromatography (HPLC) method for separation and analysis of TDL from rat plasma was developed. Chromatography was performed on Jasco LC 1500 coupled with UV detector (Jasco UV/VIS 1570/1575), a 100 μl injection loop with Rheodyne injector (model 7725) Spherisorb®C18 column ODS2 (5 μm, 4.6 mm × 250 mm, Waters, USA) analytical column. Chromatography was performed at room temperature under isocratic condition comprised of Acetonitrile: Phosphate buffer

pH 3 (50:50) at a flow rate of 1.2 ml/min with UV detection at 285 nm. TDL from plasma was extracted by protein precipitation using Acetonitrile. Briefly, 500 µl of Acetonitrile was added to 200 µl plasma, vortex mixed and sonicated for 5 min, followed by centrifugation at 15,000 rpm for 20 min and the supernatant (100 µl) was assayed using HPLC. Plasma TDL concentration Vs time curve was plotted and pharmacokinetic parameters were calculated using Non-Compartmental Analysis model (Phoenix WinNonlin® software, USA).

2.13.3. *Efficacy in LPS induced pyelonephritis in rats*

Rats were randomly distributed into five groups with six rats in each group. Group I served as the normal control (sham control) and was intraperitoneally injected with normal 1 ml saline. PN was induced by single intraperitoneal injection of 1 ml of aqueous LPS solution (2 mg/ml) in animals of Groups II to V under isoflurane anesthesia on day 1. Group II served as LPS control (PN control) and administered daily by oral gavage with 0.5% w/v CMC (day 1 to 14). Groups III to V received TDL dispersed in 0.5% w/v CMC, TDL-SD (KSM0) and TDL-SMEC-SD (KSM20) dispersed in water respectively by oral gavage for 14 d at the dose equivalent to TDL 10 mg/kg body weight [3].

On 1, 7, and 14 d the body weight was monitored and blood was collected from retro-orbital plexus in two parts, in heparinized and non-heparinized tubes for plasma and serum collection respectively for estimation of blood urea nitrogen (BUN), serum creatinine and plasma nitrate/nitrite (NOx). On day 14 rats were sacrificed with an excess of CO_2 and the kidneys were excised and fixed in formalin (10%v/v) for histopathological assessment.

The BUN and serum creatinine were estimated using commercially available diagnostic kits. Plasma NOx was estimated using previously described a spectrophotometric method using Griess reagent as a colour reagent and vanadium (III) as reducing agent [18]. Briefly, Griess reagent (100 µl) and deproteinized plasma sample (100 µl) were added to 96-wells plate followed by addition of 100 µl of vanadium (III) in 1 M HCl to each well and measurement of UV absorbance at 540 nm using microplate reader.

2.14. *Statistical analysis*

The data are expressed as the mean ± SD. The statistical significance of the difference in each parameter among the groups was evaluated using one-way analysis of variance (ANOVA) followed by Dunnett's post-ANOVA test. The criterion for the statistically significant difference was chosen to be at $P < 0.05$.

3. Results and discussion

3.1. *Calculation of thermodynamic parameters*

To ensure that the same polymers and SMEC components studied for curcumin would be appropriate for TDL, thermodynamic parameters for TDL with the polymers KVA, HPMC, Eudragit EPO and SMEC, namely total solubility parameter (δ_{total}), mixing enthalpy (ΔH_M) and polarity (ΔPol) were determined.

Total solubility parameter (δ_{total}) is the net effect of intermolecular and intramolecular forces which could include electrostatic interaction, ionic interaction, Van der Waals interaction and hydrogen bonding [19]. $\Delta\delta_{total}$ is an indicator of the affinity of two components, with a low $\Delta\delta_{total}$ reflecting greater affinity. Among the various polymers, minimum and low $\Delta\delta_{total}$ exhibited by TDL with KVA indicated high affinity. The significantly higher $\Delta\delta_{total}$ with the other polymers reflected lower affinity (Table 2).

The mixing enthalpy (ΔH_M) a thermodynamic parameter is an indicator of the energy required for spontaneous mixing of two components with a low value of ΔH_M suggesting spontaneous mixing. The ΔH_M value of the polymers could not be predicted due to their multiple 3-D structures, and hence was evaluated only with plasticizers (Table 2). ΔH_M of TDL with SMEC suggested a good affinity.

ΔPol which characterizes the difference in polarity is yet another parameter which indicates affinity between two components. Closer polarity between two components lowers the ΔPol and greater the affinity. The polarity of TDL and KVA was very close (ΔPol = 0.17) suggesting high affinity of TDL and KVA. ΔPol was significantly higher with HPMC (0.28) reflecting low interaction (Table 2). Although ΔPol was zero for TDL and Eudrgit EPO, a high $\Delta\delta_{total}$ indicated lower affinity. In the case of SMEC, the ΔPol value was negligible (~0.02) suggesting high affinity of TDL for SMEC.

The thermodynamic parameters confirmed the high affinity of TDL to KVA among the polymers. The high affinity to SMEC was confirmed by the high solubility of TDL in SMEC (45.61 mg/ml) proposing TDL as a suitable candidate for

Table 2 – Thermodynamic parameters for Tadalafil and excipients.

Ingredients	Solubility parameters					Polarity values	ΔPol	Mixing enthalpy
	δ_d (MPa$^{1/2}$)	δ_p (MPa$^{1/2}$)	δ_h (MPa$^{1/2}$)	δ_{total} (MPa$^{1/2}$)	$\Delta\delta_{total}$ (MPa$^{1/2}$)			
Tadalafil	28.68	12.22	10.98	33.05		0.25	–	–
Kollidon VA64	20.20	12.20	11.86	26.41	6.64	0.41	0.17	–
HPMC[a]	14.65	4.57	14.93	21.41	11.64	0.53	0.28	–
Eudragit EPO	17.55	3.43	9.46	20.23	12.82	0.25	0.00	–
SMEC[b]	17.68	1.11	10.61	20.65	12.40	0.27	0.02	14.92

[a] Hydroxypropyl methyl cellulose.
[b] Self micro-emulsifying composition.
δ_d, δ_p, and δ_h are partial solubility parameter associated with dispersion forces, polar interaction and hydrogen bonding, respectively. δ_{total} = Total solubility parameter; $\Delta\delta_{total}$ = difference between total solubility parameter. ΔPol = difference between polarity.

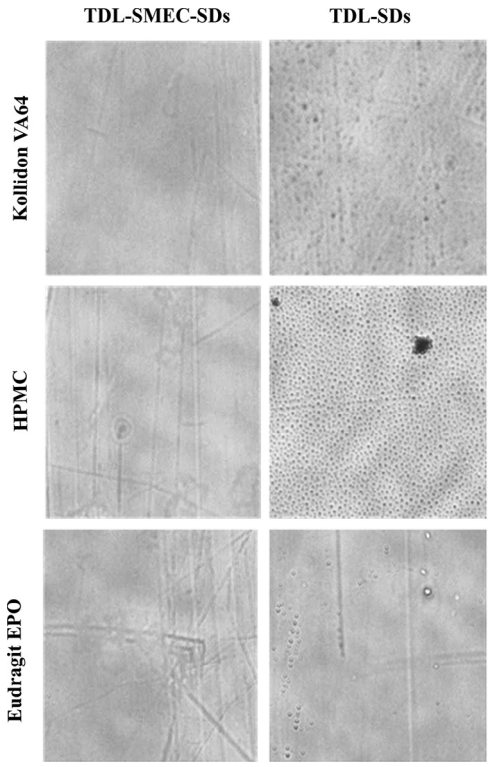

Fig. 1 – Polarizing microscope images of TDL loaded polymeric films (A) TDL-SMEC-SDs (B) TDL-SDs.

incorporation in the advanced third generation SDs using KVA as a polymer with SMEC.

3.2. *Formulation of self micro-emulsifying composition (SMEC) of TDL*

TDL exhibited a high solubility of 45.61 mg/ml in the SMEC, with an average globule size of 117.3 ± 0.6 nm and 104.3 ± 0.4 nm at 1:10 and 1:100 dilutions respectively confirming microemulsion formation even at high dilution. The ability of the SD (with and without SMEC) to form films and retain the drug without crystallization was assessed to ensure the stability of the SD coated onto tablet core. It is also well demonstrated that amorphous TDL has a higher solubility than the crystalline drug [12,20]. TDL-SD exhibited good film formation, nevertheless the appearance of TDL crystals in less than 12h confirmed poor physical stability. TDL-SMEC-SD revealed good film formation with no crystallization evident even after 72 h, indicating superior stability attributed to the formation of a solid solution/amorphization of TDL (Fig. 1). This proposed enhancement in TDL solubility, as amorphous TDL is predicted to exhibit higher solubility than the crystalline form [12,20].

3.3. *Differential scanning calorimetric (DSC) and x-ray powder diffraction (XRD)*

A sharp endotherm of TDL at 300 °C corresponding to its melting point evident in TDL-SD (KSM0) was absent in the TDL-SMEC-SD thermograms signifying solubilization of TDL (Fig. 2). Further, the XRD data correlated well with the DSC results (Fig. 3). While

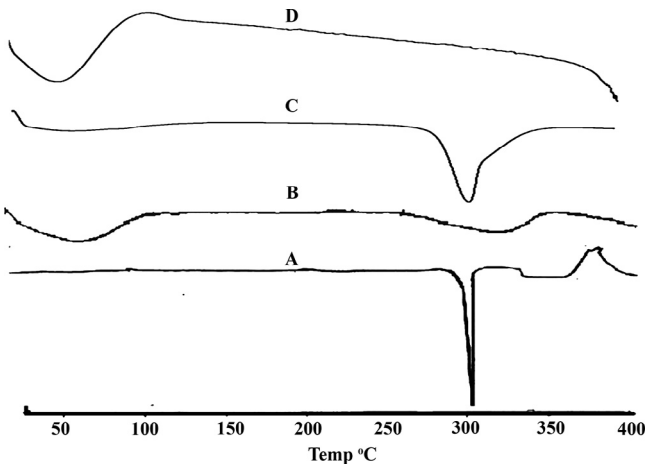

Fig. 2 – DSC profile of (A) Plain TDL (B) KVA TDL-SMEC-SDs (KSM20) (C) KVA TDL-SD (KSM0) (D) KVA.

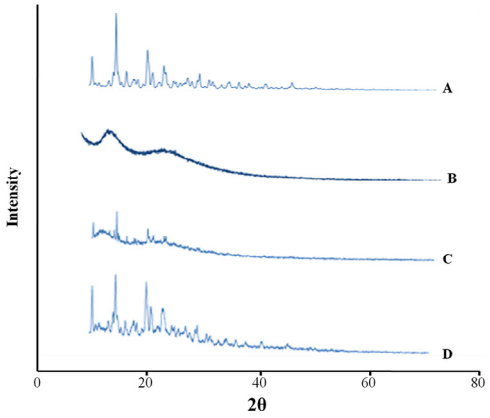

Fig. 3 – Powder X-ray diffraction patterns of (A) Plain TDL (B) KVA (C) KVA TDL-SMEC-SDs (KSM20) (D) KVA TDL-SDs (KSM0).

typical TDL diffraction peaks were observed in the diffractograms of TDL and TDL-SD (KSM0), the peaks were absent in TDL-SMEC-SD (KSM20) confirming that TDL was either in solubilized or amorphous form. The TDL-SMEC-SD was therefore considered suitable for coating onto inert tablet cores.

3.4. *TDL-SMEC-SD loaded tablets*

A dose of 20 mg of TDL per tablet was readily achieved by spray coating on the inert tablet cores. A barrier coating of HPMC was applied to overcome tackiness during storage. (CUR REF) TDL-SMEC-SD coated tablets exhibited hardness of 4.0 – 5.0 kg/cm^2 and complied with requirements of weight variation (250 mg ± 3%), assay (98–101%), disintegration (≤2 min) and friability (<1%).

When introduced into aqueous media, the inert cores disintegrated rapidly to release the TDL-SMEC-SD as films. The films comprising ~20 mg of TDL weighed about 44 mg with an approximate thickness and surface area of 100 μ and 2.39 cm^2, respectively. As obtained with curcumin a high loading of up to 45% of TDL was achieved in the SMEC SD. TDL-SMEC-SD facilitated rapid release of TDL, compared to TDL-SD which

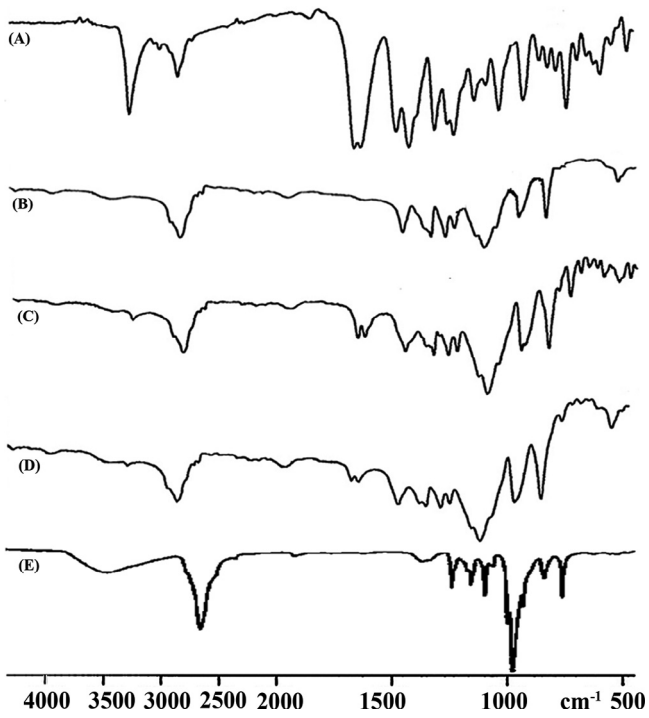

Fig. 4 – FTIR spectra of (A) Plain TDL (B) KVA TDL-SMEC-SDs (KSM20) (C) KVA TDL-SDs (KSM0) (D) HPMC TDL-SMEC-SDs (HSM20) (E) Eudragit EPO TDL-SMEC-SDs (EPSM20).

revealed slower dissolution (Fig. 6). More importantly, microemulsion formation was exhibited by the TDL-SMEC-SD, with average globule size 108 nm and PDI 0.173. ME formation was also confirmed by observing the filtered solutions through an optical polarizer which revealed isotropy.

3.5. *Fourier transform infrared spectroscopy (FTIR)*

FTIR spectrum of pure TDL (Fig. 4) showed an intense, well-defined characteristic infrared absorption band at 3323 cm^{-1} (N-H secondary amine stretching) and 3057 cm^{-1} (C–H aromatic stretching). Two intense absorption bands associated with the carbonyl stretching vibration were found at 1675 cm^{-1} (C = O amide) and 1647 cm^{-1} (C-C aromatic). Additionally, other sharp bands at 2900 cm^{-1} (C–H aliphatic stretching), 1500–1400 cm^{-1} (C–C aromatic stretching) and 1239 cm^{-1} (C–N stretching) were also present.

In presence of SMEC, the stretching vibrations of secondary amine groups (3323 cm^{-1}) and carbonyl groups (1675 cm^{-1} and 1647 cm^{-1}) of TDL, were absent when KVA and Eudragit EPO were the polymers in the SD. However, the signals of lower intensity were seen with HPMC as polymer and in the absence of SMEC. This suggested interaction of TDL with KVA and Eudragit EPO in the presence of SMEC.

3.6. *Scanning electron microscopy*

SEM photographs of TDL-SMEC-SD (KSM20) revealed smooth, continuous, homogenous and uniform films with no evidence of crystallization of TDL, even at the end of 3 months (Fig. 5A). However, tablets coated with TDL-SD revealed crystals of TDL and cracks in the film (Fig. 5B). SMEC, therefore, appears to contribute as a solubilizer and as a crystallization inhibitor in the advanced third generation SDs thereby enabling high TDL loading coupled with enhanced physical stability.

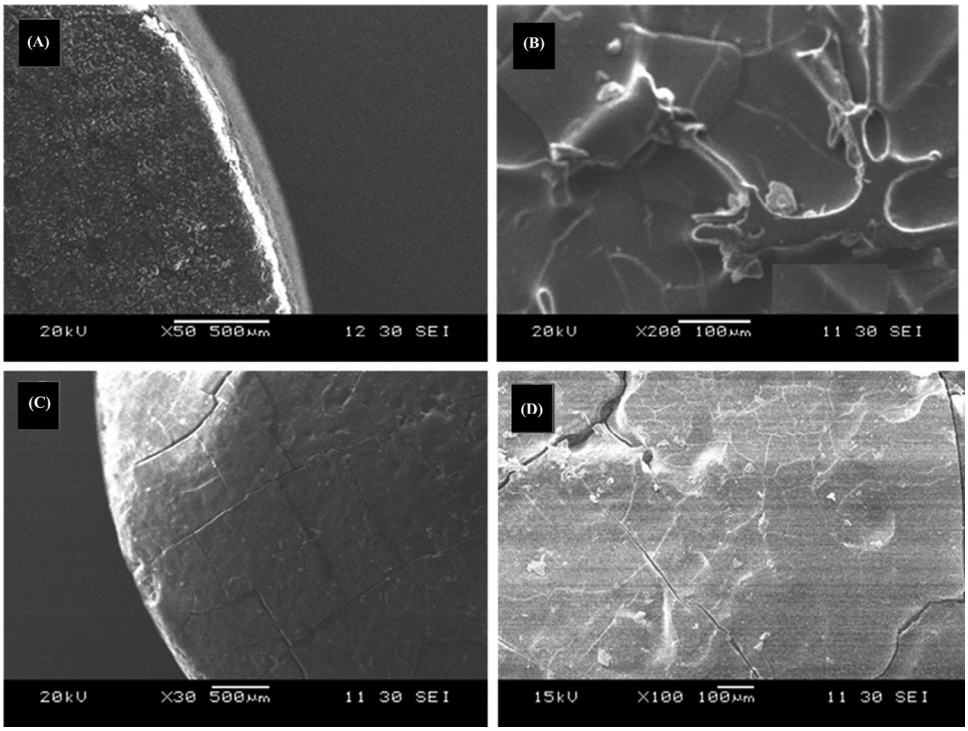

Fig. 5 – Scanning electron micrographs of (A& B) TDL-SMEC-SD tablets (KSM20) (C & D) TDL-SD tablet (KSM0).

Table 3 – Mathematical models after curve fitting of in-vitro drug release data of TDL-SMEC-SDs using different polymers ($n = 6$).

Formulations	R^2 Values for mathematical models				
	First order	Zero order	Higuchi	HixenCrowel	Korsmeyer
KSM20[a]	0.999	0.789	0.921	0.935	0.993
HSM20[c]	0.995	0.891	0.997	0.945	0.927
EPSM20[b]	0.991	0.902	0.925	0.912	0.955

TDL-SMEC-SDs using [a]Kollidon VA64, [b]Eudragit EPO and [c]hydroxypropyl methyl cellulose.

3.7. *Contact angle measurement*

While TDL-SD (KSM0) revealed a very high contact angle of 114°, although the TDL-SMEC-SD revealed significant decrease in contact angle, attributed to the high hydrophilicity and surface active property of SMEC, the same contact angle was significantly influenced by the polymer in the SD, as seen from the values; HPMC (16°), Eudragit EPO (11°), and KVA (9°). These differences are attributed to the hydrophilic nature of the polymers and the interactions of SMEC with the polymers as elucidated by FTIR. The minimum contact angle was seen with KVA.

3.8. *In-vitro drug release*

Among the SDs, the exceptionally rapid release was observed with KVA as a polymer (KSM20) with very low t_{50} (7.3 min) and t_{90} (30.2 min). The significantly slower release was seen with all other polymers and was in the order EPO > HPMC (Fig. 6). This data corroborated with our earlier observation for curcumin as a drug and is attributed to the molecular weight and viscosity of the polymers, wherein greater the molecular weight, higher the viscosity and slower the release [16,21]. A decrease in SMEC concentration (KSM10) resulted in significant increase in t_{50}, but increase to 30% (KSM30) exhibited no significant change in dissolution profile (F2 value 65.88) suggesting 20% SMEC as optimal. In the absence of SMEC, TDL-SD revealed significantly slower dissolution with a very high $t_{50}$of greater than 70 min. The release kinetic model fitting is reported in Table 3. Five models were evaluated and it was observed that KVA and Eudragit EPO SMEC-SDs displayed first order kinetics while HPMC SMEC- SD exhibited Higuchi kinetics.

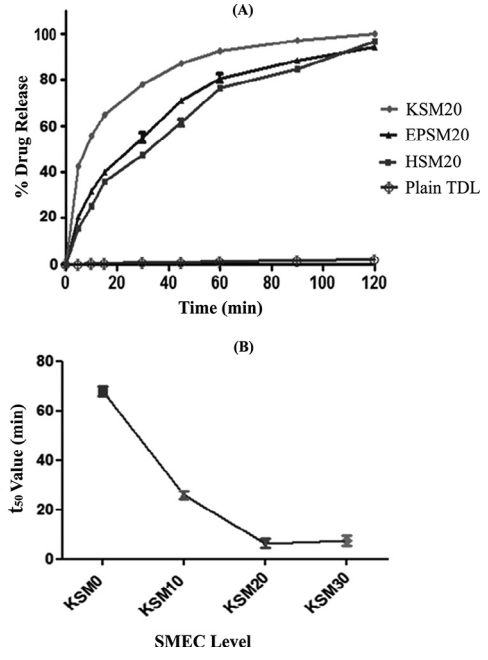

Fig. 6 – In vitro release in simulated gastric fluid (SGF) pH 1.2 (A) Effect of polymer (B) effect of SMEC concentration.

3.9. *Stability studies*

The formulation KSM20 (TDL-SMEC-SD) exhibited good stability with no change in hardness, friability and weight variation (Table 4). Drug content was greater than 98% even after storage at 40 °C ± 2 °C, 75 ± 5% RH for 6 months. Further, no significant difference in drug release ($F_2 > 50$) and average globule size ~100 nm suggested good stability.

3.10. *Pharmacokinetic study*

Table 5 and Fig. 7A confirmed the rapid absorption and enhanced bioavailability with TDL-SD. Although t_{max} was comparable (1h), C_{max} was in the order TDL < TDL-SD (KSM0) < TDL-SMEC-SD (KSM20) and was significantly higher than the plain TDL ($P < 0.05$). Enhanced bioavailability with TDL–SDs (KSM0) is attributed to rapid dissolution of TDL from the SDs favored by improved wetting and amorphization [13]. Nevertheless, the greater enhancement seen with TDL-SMEC-SD (KSM20) is due to the formation of the microemulsion in an aqueous medium, confirms the role of SMEC in superior bioenhancement [22,23]. Further, mean residence time of

Table 4 – Stability data of TDL-SMEC-SDs (KSM20) (Mean ± SD; $n = 3$).

Sampling time	Globule size (nm) ($n = 3$)	Assay (%) ($n = 3$ sets)	T_{50} (min) ($n = 6$)	F2Value ($n = 6$)
Initial	101.7 ± 7.4	96.7 ± 1.2	7.3	Reference
30 °C/65%RH				
1 month	102.1 ± 3.2	97.1 ± 2.3	7.1	73.2
3 month	105.1 ± 2.5	96.8 ± 2.5	7.4	69.5
6 month	111.4 ± 5.5	96.9 ± 4.3	7.3	73.0
12 months	104.1 ± 1.1	97.1 ± 3.4	7.8	69.1
45 °C/75%RH				
1 month	111.4 ± 1.3	97.2 ± 2.7	7.5	68.1
3 month	100.1 ± 0.5	96.9 ± 5.3	8.1	71.4
6 month	108.2 ± 0.9	96.8 ± 0.7	7.5	72.2

Table 5 – Pharmacokinetic parameters after oral administration of Tadalafil (TDL) formulations. (Data expressed as Mean ± SD; n = 4).

Parameters	TDL	TDL-SD (KSM0)	TDL-SMEC-SD (KSM20)
Cmax (μM)	2.4 ± 0.1	3.6 ± 0.4	5.8 ± 0.3
Tmax (h)	1.2 ± 0.5	0.8 ± 0.3	0.9 ± 0.2
$T_{1/2}$ (h)	3.0 ± 0.5	4.2 ± 0.8	5.3 ± 0.6
$AUC_{0-\infty}$ (μM*h)	12.8 ± 4.0	22.9 ± 5.8	42.4 ± 6.2
AUC0-t (μM*h)	12.1 ± 4.1	22.3 ± 5.4	40.7 ± 5.9
MRT (h)	4.7 ± 1.1	6.4 ± 1.3	7.8 ± 0.7
Relative bioavailability (%)	–	178.9	330.6

TDL-SMEC-SD (KSM20) was also significantly higher than the TDL-SD (KSM0) and plain TDL (Fig. 7A).

3.11. *Efficacy in LPS-induced pyelonephritis in rats*

Pyelonephritis is a specific type of urinary tract infection that generally begins in the urethra or bladder and travels up into the kidneys. If not treated properly, this infection can cause permanent damage to the kidneys. Moreover, the bacteria can spread to the bloodstream and cause life-threatening infection [24,25]. Elevated levels of blood urea nitrogen (BUN), plasma nitric oxide and serum creatinine associated with Pyelonephritis were retained as biomarkers to monitor the efficacy of the TDL SDs. Plasma NO levels were monitored indirectly by measuring the oxidative products namely nitrate and nitrite (NOx). As expected, decreased levels of BUN, NO (plasma NOx) and serum creatinine were exhibited by TDL, indicating its efficacy in PN (Fig. 7B and 7C). Nevertheless, these levels were significantly higher than the normal untreated group. Although the TDL SDs revealed significantly greater inhibition than TDL ($P < 0.05$), the TDL-SMEC-SD (KSM20) revealed significantly greater inhibition ($P < 0.05$) of all the biomarkers compared to TDL-SD (KSM0).

Microscopic examination showed histological changes namely interstitial inflammatory cell infiltration and tubular dilatation, and interstitial fibrosis/tubular atrophy (IF/TA; scar tissue) related to activation of local cellular mediators of inflammation in the PN control group (Fig. 8). Reduction in tubular degeneration and multifocal infiltration of inflammatory cells and interstitial fibrosis was significantly lowered with

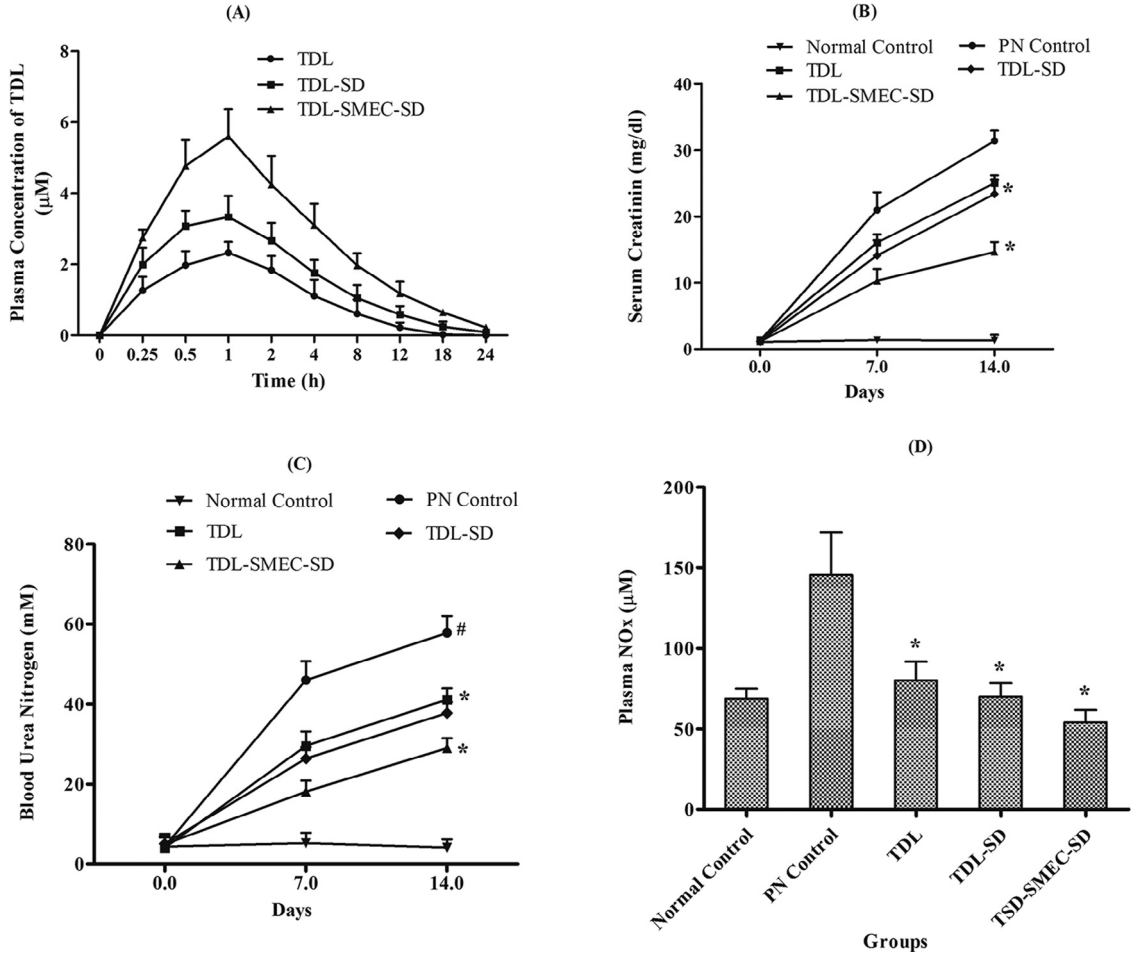

Fig. 7 – (A) Plasma concentration vs. time profiles after oral administration of TDL formulations (n = 4); Effect of chronic treatment on levels of (B) Serum Creatinine, (C) Blood urea nitrogen and (D) plasma NOx in LPS-injected pyelonephritic rats (*n* = 6). *P < 0.05 compared with pyelonephritis control;#P < 0.05 compared with normal control using One-way ANOVA All values reported are Mean ± SD.

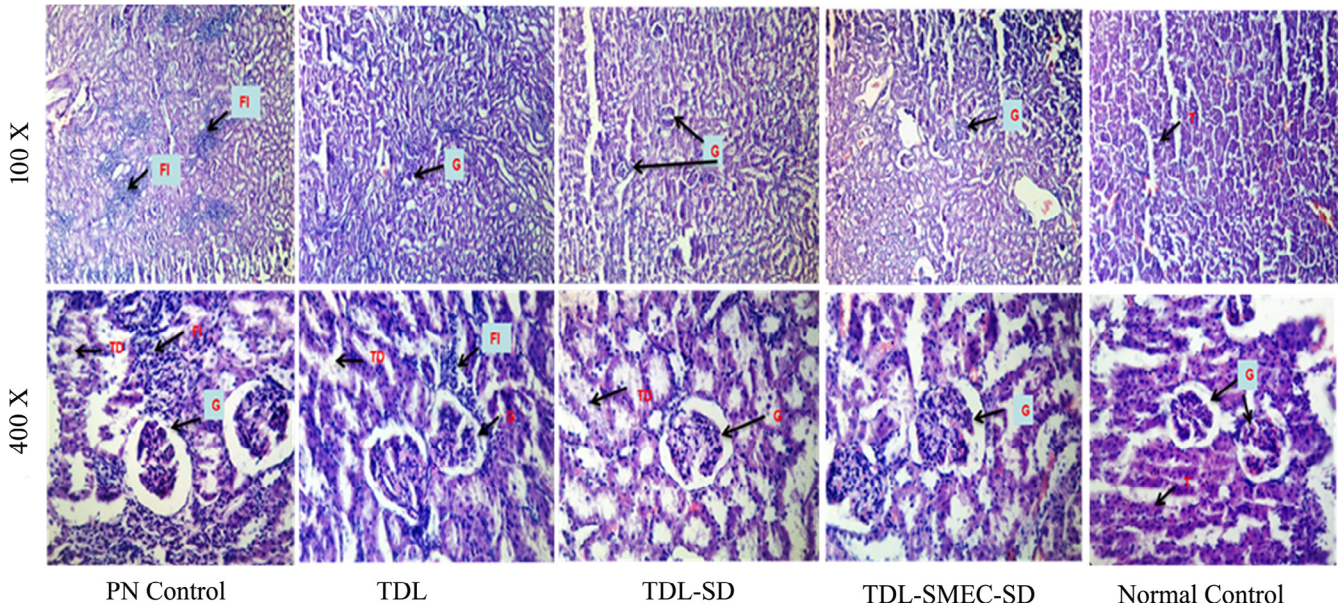

Fig. 8 – Histopathology of rat kidney showing prevention of morphological and inflammatory changes by Tadalafil in pylonephritic rats.

TDL-SMEC-SD (KSM20) compared to TDL-SD (KSM0) and TDL. Furthermore, unlike the other two groups, TDL-SMEC-SD group showed significant recovery in weight loss to achieve weight comparable to control group ($P > 0.05$), indicating the superiority of TDL-SMEC-SD (KSM20).

4. Conclusion

The study proposes TDL for efficacious therapy of PN through the design of TDL-SMEC-SD, a bioenhanced formulation of TDL. The simplicity of technology and the high stability of TDL-SMEC SD suggest the great promise of repurposing TDL for improved therapy of PN through this new drug delivery system.

Conflicts of interest

The authors declare that there are no conflicts of interest.

Acknowledgments

The authors acknowledge the financial support received from Phoenix Pharmaceuticals LLC, USA, for providing research fellowship.

REFERENCES

[1] Carvalho ALSL, de Araújo NAB, Lima RH, et al. Tadalafil and its effects in renal function after kidney ischemia and reperfusion in rats. J Surg Cl Res 2015;6:22–30.

[2] Kyriazis I, Kagadis GC, Kallidonis P, et al. PDE5 inhibition against acute renal ischemia-reperfusion injury in rats: does vardenafil offer protection? World J Urol 2013;31:597–602.

[3] Zhu CY, Liu M, Liu YZ, et al. Preventive effect of phosphodiesterase 5 inhibitor tadalafil on experimental post-pyelonephritic renal injury in rats. J Surg Res 2014;186:253–261.

[4] Krupa A, Descamps M, Willart J-F, et al. High-energy ball milling and supercritical carbon dioxide impregnation as co-processing methods to improve dissolution of tadalafil. Eur J Pharm Sci 2016;1:130–137.

[5] Obeidat WM, Sallam ASA. Evaluation of Tadalafil nanosuspensions and their PEG solid dispersion matrices for enhancing its dissolution properties. AAPS PharmSciTech 2014;15:364–374.

[6] Badr-Eldin SM, Elkheshen SA, Ghorab MM. Inclusion complexes of tadalafil with natural and chemically modified beta-cyclodextrins. I: preparation and in-vitro evaluation. Eur J Pharm Biopharm 2008;70:819–827.

[7] Mehanna MM, Motawaa AM, Samaha MW. Tadalafil inclusion in microporous silica as effective dissolution enhancer: optimization of loading procedure and molecular state characterization. J Pharm Sci 2011;100:1805–1818.

[8] Bhokare PL, Kendre PN, Pande VV. Design and characterization of nanocrystals of Tadalafil for solubility and dissolution rate enhancement. Inventi Rapid 2015;3:1–7.

[9] El-Badry M, Haq N, Fetih G, et al. Solubility and dissolution enhancement of tadalafil using self-nanoemulsifying drug delivery system. J Oleo Sci 2014;63:567–576.

[10] Leuner C, Dressman J. Improving drug solubility for oral delivery using solid dispersions. Eur J Pharm Biopharm 2000;50:47–60.

[11] Serajuddin ATM. Solid dispersion of poorly water-soluble drugs: early promises, subsequent problems, and recent breakthroughs. J Pharm Sci 1999;88:1058–1066.

[12] Wlodarski K, Sawicki W, Haber K, et al. Physicochemical properties of tadalafil solid dispersions – Impact of polymer on the apparent solubility and dissolution rate of tadalafil. Eur J Pharm Biopharm 2015;94:106–115.

[13] Vyas V, Sancheti P, Karekar P, et al. Physicochemical characterization of solid dispersion systems of tadalafil with poloxamer 407. Acta Pharm 2009;59:453–461.
[14] Vasanthavada M, Tong WQ, Joshi Y, et al. Phase behavior of amorphous molecular dispersions I: determination of the degree and mechanism of solid solubility. Pharm Res 2004;21:1598–1606.
[15] Baghel S, Cathcart S, O'Reilly NJ. Polymeric amorphous solid dispersions: a review of amorphization, crystallization, stabilization, solid-state characterization, and aqueous solubilization of biopharmaceutical classification system class II drugs. J Pharm Sci 2016;105:2527–2544.
[16] Mande PP, Bachhav SS, Devarajan PV. Solid dispersion of curcumin as polymeric films for bioenhancement and improved therapy of rheumatoid arthritis. Pharm Res 2016;33:1972–1987.
[17] van Krevelen DW, Nijenhuis K. Properties of polymers: their correlation with chemical structure; their numerical estimation and prediction from additive group contributions. 4th ed. Amsterdam: Elsevier Science; 2009. p. 322.
[18] Miranda KM, Espey MG, Wink DA. A rapid, simple spectrophotometric method for simultaneous detection of nitrate and nitrite. Nitric Oxide 2001;5:62–71.
[19] Jindal AB, Devarajan PV. Asymmetric lipid-polymer particles (LIPOMER) by modified nanoprecipitation: role of non-solvent composition. Int J Pharm 2015;489:246–251.
[20] Parka J, Choa W, Kanga H, et al. Effect of operating parameters on PVP/tadalafil solid dispersions prepared using supercritical anti-solvent process. J Supercrit Fluids 2014;90:126–133.
[21] Zeng Z, Sun L, Xue W, et al. Relationship of intrinsic viscosity to molecular weight for poly (1, 4-butylene adipate). Polym Test 2010;29:66–71.
[22] Cerpnjak K, Zvonar A, Gašperlin M, et al. Lipid-based systems as a promising approach for enhancing the bioavailability of poorly water-soluble drugs. Acta Pharm 2013;63:427–445.
[23] Tarr BD, Yalkowsky SH. Enhanced intestinal absorption of cyclosporine in rats through the reduction of emulsion droplet size. Pharm Res 1989;6:40–43.
[24] Lin KY, Chiu NT, Chen MJ, et al. Acute pyelonephritis and sequelae of renal scar in pediatric first febrile urinary tract infection. Pediatr Nephrol 2003;18:362–365.
[25] Oh MM, Kim JW, Park MG, et al. The impact of therapeutic delay time on acute scintigraphic lesion and ultimate scar formation in children with first febrile UTI. Eur J Pediatr 2012;171:565–570.